Anomalous behavior of the acoustic phonon velocity and elastic constants of relaxor ferroelectric $PbMg_{1/3}Ta_{2/3}O_3$

S. G. Lushnikov[1&], A.I.Fedoseev[1], S.N.Gvasaliya[2,*], J.-H. Ko[3], Seiji Kojima[4]

[1] *Ioffe Physico-Technical Institute of Russian Academy of Sciences, 194021 St.Petersburg, Politekhnicheskaya str., 26, Russia*

[2]*Laboratory for Neutron Scattering, ETH Zurich & Paul Scherrer Institut, CH-5232 Villigen PSI, Switzerland*

[3]*Department of Physics, Hallym University, 39 Hallymdaehakgil, Chuncheon, Gangwondo 200-702, Korea*

[4]*Institute of Materials Sciences, University of Tsukuba, Tsukuba, Ibaraki, 305-8573 Japan*

sergey.lushnikov@mail.ioffe.ru

The behavior of longitudinal (LA) and transverse (TA) acoustic phonons in a cubic relaxor $PbMg_{1/3}Ta_{2/3}O_3$ (PMT) ferroelectric has been investigated by Brillouin light scattering. Analysis of the temperature dependences of phonon velocity in the temperature range from 50 to 870 K has revealed anomalies in the vicinity of Burns temperature ($T_B \approx 570$K) for LA phonons and a wide frequency-dependent minimum of the velocities of LA and TA phonons in the same temperature region as the dielectric response anomaly. Using experimental data, temperature dependences of the C_{11} and C_{44} elastic constants have been calculated. The elastic constants have been found to be frequency-independent in the gigahertz range. The results obtained are discussed in the framework of modern ideas on the crystalline lattice dynamics of relaxor ferroelectrics.

PACS numbers: 62.65.+k, 77.84.Dy, 77.84.-s, 78.35.+c, 77.22.Gm

[&] Author to whom any correspondence should be addressed.

[*] On leave from: Ioffe Physico-Technical Institute of Russian Academy of Sciences, 194021 St.Petersburg, Politekhnicheskaya str., 26, Russia

The relaxor state that arises in a number of disordered ferroelectric crystals has been a subject of intense investigations during the last decades [1-4]. The interest of researchers to this state is due to the importance of the problem of the dynamics of structural phase transitions in partially disordered crystals (one of the sublattices is partially disordered) and also due a wide use of relaxor ferroelectrics in industry.

Crystals of lead magnesium tantalate $PbMg_{1/3}Ta_{2/3}O_3$ (PMT) are representatives of a large family of relaxor perovskite-like ferroelectrics with the common formula $AB'B''O_3$ [5]. Though the parent compound of relaxor ferroelectrics (from here on - relaxors) is classical ABO_3 perovskites, the relaxors exhibit the properties radically differing from those of the parent compound. For instance, the dielectric response of PMT demonstrates a frequency-dependent anomaly spread for several hundred degrees with a maximum at $T_0 \approx 170$ K at 10 kHz [6]. In contrast to classical ferroelectrics, the anomalies in the dielectric response of relaxors are not directly associated with a structural phase transition. The X-ray and neutron diffraction analyses of PMT crystals have revealed the absence of a structural phase transition in the range of temperatures from 1.5 to 730 K [7-9], which is also typical of related relaxor compound $PbMg_{1/3}Nb_{2/3}O_3$ (PMN). However, in contrast to PMN, the PMT crystals remain cubic (with the $Pm\bar{3}m$ symmetry) even if an external electric field is applied [5, 9]. The absence of a structural instability makes PMT crystals suitable model objects for studies of the relaxor ferroelectric state. The crystalline lattice dynamics of PMT crystals has been investigated by dielectric, optical, and neutron spectroscopy [6, 10-13] and specific heat measurements [14]. Inelastic neutron scattering experiments have revealed that characteristic features of the low-frequency region of the vibration spectrum of cubic relaxor ferroelectrics are a narrow central peak and a relaxation mode (quasi-elastic scattering - QE) [13, 15-18]. At the temperature at which the QE scattering, arises damping of the low-energy phonons starts to increase, which may be a consequence of the scattering by dynamic polar nanoregions [17, 18]. Thetemperature evolution of optical phonons in PMT was studied by Raman scattering in Ref. [10]. It was found that the integrated susceptibilities of the phonon peaks exhibit an anomalous behavior in the range of a strong frequency dispersion of the dielectric permittivity of PMT. In addition, the Raman line shape of the high-frequency phonon in PMT becomes more asymmetric at temperatures lower than T_0. The first results of the studies of the behavior of longitudinal acoustic phonons in PMT and their comparison with the behavior of longitudinal acoustic phonons in $PbMg_{1/3}Nb_{2/3}O_3$ and $BaMg_{1/3}Ta_{2/3}O_3$ were reported in [6]. However, to our knowledge, no thorough studies of the behavior of acoustic phonons in $PbMg_{1/3}Ta_{2/3}O_3$ have been carried out so far. For this reason, detailed investigations of the behavior of acoustic phonons in PMT crystals are of high importance.

This paper discusses the data for a PMT crystal obtained in Brillouin light scattering experiments in the temperature range from 870 to 50 K including both the region of formation of polar nanoregions $T_B \approx 570$ K [6,9] (which are believed to be responsible for the relaxor state [19]) and the region of the anomalous behavior of the dielectric response.

The Brillouin scattering measurements in the PMT crystal involved the use of a 3+3-pass Fabry-Perot interferometer (J.Sandercock tandem) with an optical microscope. A source of scattered light excitation was an Ar^+-ion laser with a wavelength $\lambda_0 = 514.5$ nm. The radiation power was not higher than 100 mW. Two scattering geometries were used: 90˚ and 180˚. In the case of a 180˚-geometry, the samples were mounted in an optical cell (THMS 6000) where temperature was varied from 870 to 80 K with a stabilization of ± 0.1 °K. In the 90˚- geometry, a furnace and an optical cryostat where temperature variations were controlled with the same accuracy and in approximately the same temperature range with the help of a digitized temperature controller (SI9650/Lakeshore331) and a closed-cycle helium refrigerator (RMC LTS-22), respectively, were used. Note that in the experiments described above, the same PMT crystal as in Raman light scattering and inelastic neutron scattering experiments was used [10,12,13]. The crystal was in the form of a parallelepiped 6.5 × 4.5 × 1.6 mm^3 in size whose polished faces were oriented along the [100], [010], and [001] directions. The error in the sample orientation accomplished with an X-ray diffractometer was less than 1˚.

The acoustic phonon velocity (V) in a Brillouin light scattering experiment is determined by the frequency shift ($\Delta\nu$) as

$$Vq = \omega = 2\pi\Delta\nu, \qquad (1)$$
$$q = (4\pi n/\lambda_0)\sin(\theta/2),$$

where q, n, and θ are the wave vector, refractive index, and the angle between the incident and scattered light, respectively. In the 180˚ light scattering geometry (θ=180˚), acoustic phonons with wave vector $\mathbf{q_{ph}} \| [100]$ were studied, polarizations of the incident and scattered light were oriented along [010]. Then, according to the selection rules [20], the scattering spectrum of a crystal with a cubic symmetry contains only one purely longitudinal phonon mode (LA) whose (V^a) velocity is given by

$$V_{LA}^a = \frac{\lambda_0 \Delta\nu_{LA}^a}{2n} \qquad (2).$$

Index a designates the 180˚ experimental geometry. In the 90A (θ=90˚) scattering geometry the light was incident at angle 45˚ to the crystal face (see Fig.1). In this geometry, acoustic phonons with $\mathbf{q_{ph}} \| [100]$ and polarizations of the incident and scattered light oriented along [010] were

studied. The scattering spectrum of the PMT crystal contained a purely longitudinal and a purely transverse (TA) phonon modes (Fig.2b) whose velocities V_{LA}^{b} and V_{TA}^{b} are given by

$$V_{LA}^{b} = \frac{\lambda_0 \Delta \nu_{LA}^{b}}{\sqrt{2}}; \qquad (3)$$

$$V_{TA}^{b} = \frac{\lambda_0 \Delta \nu_{TA}^{b}}{\sqrt{2}}; \qquad (4)$$

where $\Delta \nu_{LA}^{b}$ and $\Delta \nu_{TA}^{b}$ are the frequency shifts of the longitudinal and transverse acoustic phonons (index *b* denotes the 90A geometry). An important advantage of the 90A light scattering geometry is that the refractive index (whose absolute value for PMT is not known) does not affect the phonon velocity being measured in such geometry [21]. A free spectral interval of the tandem was 30 or 75 GHz.

Examples of experimental spectra are shown in Fig.2. The results were processed by the least squares method. The fitting functions in calculations of phonon line shapes and scattering at an unshifted frequency were the Lorentz and Gauss functions, respectively. It is well seen from Fig.2 that there is an additional contribution at the unshifted frequency, i.e., the quasielastic scattering described by the Lorentz function. (The behavior of the quasielastic scattering with varying temperature will be discussed elsewhere.) The temperature dependences of the frequency shifts of LA and TA modes obtained by processing the spectra are presented in Fig.3. The dependences shown in Fig.3 are seen to be typical of relaxors, i.e., a wide minimum of the frequency shift as a function of temperature is observed. In accordance with Eqs. (2-4), the frequency shift is directly proportional to the acoustic phonon velocity, and for this reason we shall consider below the behavior of the velocity rather than of the frequency shift. In the high-temperature region the velocity linearly depends on temperature. The deviation of the temperature dependence of LA phonon velocity from the linear dependence is observed in the vicinity of the temperature of polar nanoregions formation ($T_B \approx 570$ K) (Fig.3a,b). For the first time this phenomenon was associated with formation of nanoregions in analysis of Brillouin light scattering in PMN crystals [22]. Later the effect of polar nanoregions on the behavior of acoustic phonons was also revealed in relaxor compound lanthanum lead zirconate titanate [23]. The deviation of the temperature dependence of the TA phonon velocity from the linear one begins at much lower temperature, in the vicinity of 500 K (Fig.3 c). Softening of the LA phonon velocity starting in the vicinity of T_B reaches a minimum at ≈ 190 K and grows with decreasing temperature (See Figs 3,4). The minima of phonon velocities correspond to the dielectric response anomaly of the PMT crystal [6]. The magnitude of variations in the LA phonon velocity is from 3.5 to 5%, depending on the measurement frequency (below we consider the frequency dependence of velocity in more detail). Thus, on the whole, the TA phonon behavior

is similar to that of the LA phonons, though the velocity minimum in the temperature dependence of TA phonon velocity is less pronounced. The magnitude of variations in the TA phonon velocity is about 2.5 %. It is interesting to note that the behavior of the phonon velocity in PMT is similar to that in disordered crystals at phase transition into a glass-like state [24]. In it known that a characteristic feature of the transition into a glass-like phase is a strong frequency dependence of the acoustic response. This necessitated analysis of the frequency dependence of the LA phonon velocity in the PMT crystal.

Note that one can determine the elastic constant C_{11} from the velocities of the LA phonons studied in different geometries. Changes in the angle of scattering in different experimental geometries vary the wave vector of the LA phonon and, hence, the probe frequency according to Eq. (1). This allows analysis of the LA phonon behavior at frequencies $f \approx 45$ and 13 GHz (180˚ and 90A scattering geometries, respectively) in a wide temperature range. To analyze the results, we plot relative variations in the frequency shift $\delta\nu_{LA} = (\Delta\nu(T) - \Delta\nu_0)/\Delta\nu_0$ measured in different experimental geometries, where $\Delta\nu_0$ is taken to be the magnitudes of the frequency shift at T=690 K. It can be seen from Fig.4 that the temperature at which the velocity has a minimum depends on frequency: for the phonons with a probe frequency of 45 GHz the minimum is observed in the vicinity of 170 K, and for a frequency of 13 GHz a minimum is observed around 210 K. Thus, the velocity minimum shifts towards higher temperatures as the frequency of measurements decreases. The dispersion in the behavior of the LA phonon velocity in PMT in this frequency range is not typical of the frequency dependence of acoustic anomalies in the vicinity of structural phase transitions. For instance, at a ferroelectric phase transition in TGS crystals a decrease in the probe frequency leads to a shift of acoustic anomalies to a low-temperature region (a ferroelectric phase) [25]. The acoustic response in $AgNa(NO_2)_2$ crystals behaves similarly [26]. The acoustic response dispersion in the vicinity of structural phase transitions can be explained in the framework of relaxation mechanisms. In the case of the PMT and PMN relaxor ferroelectrics, a decrease in frequency leads to a shift of the velocity minimum to the high-temperature region (a paraphase), which is opposite to the velocity behavior at structural phase transitions. Thus, it can be concluded that the classical relaxation mechanism is not a determining factor in the velocity dispersion in the gigahertz region in PMN and PMT crystals. To find the mechanism responsible for velocity dispersion, additional investigations of the acoustic response of relaxors in a wide frequency range are required.

The results obtained in the Brillouin light scattering experiments allowed us to calculate elastic constants C_{11} and C_{44} (Eqs. 5-7) and plot their temperature dependences (Fig.5).

$$\rho(V_{LA}^a)^2 = C_{11}^a \qquad (5)$$

$$\rho(V_{LA}^{b})^2 = C_{11}^{b} \qquad (6)$$

$$\rho(V_{TA}^{b})^2 = C_{44}^{b} \qquad (7)$$

where ρ = 9.65 g/cm^3 [27]. Using the data for the LA phonon obtained in the 180° and 90A scattering geometries and Eqs. (2, 3), we calculated the refractive index n at T = 693 K under the assumption that the hypersound velocity dispersion is absent above the Burns temperature

$$n = \frac{\Delta\nu_{11}^{a}}{\Delta\nu_{11}^{b}\sqrt{2}} = \frac{44.83}{12.807\times\sqrt{2}} \approx 2.475\,. \qquad (8)$$

Then, using the data on the temperature behavior of relative variations in the refractive index given in [28], a temperature behavior of elastic constant C_{11}^{a} was calculated from Eq.(1). Table 1 gives elastic constants C_{11} and C_{44} obtained for PMN and PMT crystals in the Brillouin light scattering experiments performed under similar conditions, i.e., in the 180° and 90A geometries. Comparative analysis has shown that the magnitudes of C_{11} for PMT are higher than for PMN in the entire range of the temperatures studied. The values of C_{44} are similar for both crystals in the low-temperature region and differ remarkably in the high-temperature region. Comparison of the temperature evolutions of elastic constant C_{11} in the PMT crystal at different frequencies (Fig.5) has revealed that there is no dispersion of C_{11} in the gigahertz range (within the limits of measuring error and under the condition of absence of the velocity dispersion above T_B). A radically different behavior is exhibited by C_{11} in the PMN crystal: a strong dispersion of C_{11} was observed in the vicinity of the dielectric response anomaly [29].

To summarize, as evidenced by Brillouin light scattering experiments, formation of polar nanoregions in the PMT crystal leads to changes in the behavior of longitudinal acoustic phonons. A wide anomaly in the velocity of acoustic phonons has been found to correspond to the anomaly in the dielectric response of PMT. The dispersion of the velocity of longitudinal acoustic phonons, which cannot be explained by the classical relaxation mechanism, has been observed. A refractive index of PMT has been determined. The magnitudes of the C_{11} and C_{44} elastic constants of PMT have been calculated, and their temperature dependences have been plotted.

The work was supported by the grants of President of the Russian Federation (SS-1415.2003.2), Russian Foundation for Basic Research 05-02-17583. One of the authors (S.G.L.) is thankful to the JSPS Invitation Fellowship Program for Research in Japan, and to Institute of Materials Science, University of Tsukuba, for hospitality.

References

1. I. Grinberg, V.R. Cooper, and A.M. Rappe 2002 Nature, 419, 909
2. Z. Kutnjak, J. Petzelt, and R. Blinc 2006 Nature, 441, 956
3. H. Fu, R.E. Cohen 2000 Nature, 403, 283
4. G. Xu, Z. Zhong, Z.-G. Ye, G. Shirane 2006 Nature Materials, 5, 134
5. G.A. Smolenskii et al. 1984 *Ferroelectrics and Related Materials*, (Gordon and Breach, NY)
6. J.-H. Ko, S. Kojima, S.G. Lushnikov, 2003 Appl. Phys. Lett., **82**, 4128
7. Z.G. Lu, C. Flicoteaux, G. Calvarin 1996 Materials Research Bull., **31**, 445
8. M.A. Akbas and P.K. Davies 1997 J. Am. Ceram. Soc., **80**, 2933
9. S.N. Gvasaliya, B. Roessli, D. Sheptyakov, S.G. Lushnikov, and T.A. Shaplygina 2004 Eur. Phys. J. B, **40,** 235
10. S.G. Lushnikov, S.N. Gvasaliya, and R. Katiyar 2004 Phys. Rev. B **70**, 172101; S.N. Gvasaliya, S.G. Lushnikov, B. Roessli and R. Katiyar 2004 Ferroelectrics, **302** 593
11. S.N. Gvasaliya, S.G. Lushnikov, I.L. Sashin, and T.A. Shaplygina 2003 J. Appl. Phys., **94**, 1130
12. S.N. Gvasaliya, B. Roessli, S.G. Lushnikov 2003 Europhys. Lett., **63**, 303
13. S.N. Gvasaliya, S.G. Lushnikov, B. Roessli 2004 Crystallography Report, **49**, 108
14. Y. Moriya, H. Kawaji, T. Tojo, and T. Atake 2003 Phys. Rev. Lett., **90**, 205901
15. S.N. Gvasaliya, S.G. Lushnikov, B. Roessli 2004 Phys.Rev. B, **69**, 092105
16. C. Stock, R.J. Birgeneau, S. Wakimoto, J.S. Gardner, W. Chen, Z-G. Ye and G. Shirane 2004 Phys. Rev. B **69** 094104
17. S.N. Gvasaliya, B. Roessli, R.A. Cowley, P. Huber, S.G. Lushnikov 2005 J.Phys.: Condens.Matter, 17 4343
18. S.N. Gvasaliya, B. Roessli, R.A. Cowley, Seiji Kojima, and S.G. Lushnikov 2007 J.Phys.: Condens.Matter, 19, 016219

19. G. Burns and F. Dacol 1983 Solid State Commun. **48**, 853

20. R. Vacher and L. Boyer 1972 Phys. Rev. **B6** 639

21. J.M. Vaughan 1989 *The Fabry-Perot Interferometer* (Adam Hilger, Bristol and Philadelphia)

22. S.D. Prokhorova and S.G. Lushnikov 1989 Ferroelectrics, **90,** 187

23. G, Shabbir, J.-H. Ko, S.Kojima, O.-R. Yin 2003 Appl. Phys. Lett. **82** 4696

24. U.T, Höchli, K. Knorr and A. Loidl 1990 Adv.Phys. **39**, 405

25. T. Yagi, M. Tokunaga, I. Tatsuzaki 1976 J. Phys.Soc. Jpn. 40, 1659

26. V.P. Soprunyuk, A. Fuith, H. Kabelka, et.al. 2002 Phys.Rev.B, 66, 104102

27. V. A. Bokov and I. E. Myl'nikova 1961 Fiz. Tverd. Tela (Leningrad) **3**, 841 [1961 Sov. Phys. Solid State **3**, 613]

28. O.Yu. Korshunov, P.A. Markovin, and R.V. Pisarev 1992 Ferroelectrics **13**, 137

29. S.G. Lushnikov, A.I. Fedoseev, S.N. Gvasaliya and Seiji Kojima (unpubished)

Table 1. Elastic constants of PMT and PMN crystals

	PMT			*PMN		
T, K	[1] C_{11}^E, Gpa	[2] C_{11}^E, GPa	C_{44}^E, Gpa	[1] C_{11}^E, GPa	[2] C_{11}^E, GPa	C_{44}^E, GPa
800	206.11	206.91	68.196	179.08	174.16	71.018
700	209.25	209.55	69.414	180.67	176.27	72.193
600	211.67	211.52	69.924	180.11	175.86	72.211
500	212.65	212.04	70.796	177.02	173.28	72.071
400	209.87	209.19	71.105	169.53	166.13	71.877
300	202.49	204.83	69.678	162.78	155.45	68.387
200	197.57	198.03	68.270	164.65	157.40	68.096
100		202.83	69.396	170.22	161.46	69.471

[1] C_{11}^E - the magnitude of the elastic constant is obtained in the experiments with the 180˚ scattering geometry, $\mathbf{q}_{ph} \| [100]$.
[2] C_{11}^E - the magnitude of the elastic constant is measured in the experiments with the 90A scattering geometry, $\mathbf{q}_{ph} \| [100]$.
* Data are taken from [29].

Figure Captions

Fig.1 Scheme of the 90A geometry of Brillouin light scattering experiment.

Fig.2 Experimental spectrum of the Brillouin light scattering at room temperature in the 180° scattering geometry (a) and 90A geometry of scattering (b).

Fig.3 Temperature dependences of the Brillouin shift for the LA phonon obtained in the 180° geometry of scattering (a) and LA and TA phonons obtained in the 90A geometry of scattering (b and c, respectively).

Fig.4 Temperature evolution of relative changes in the sound velocity of the LA phonon. Temperature variations of refractive index were taken into account in calculations of the sound velocity in the 180° geometry.

Fig.5 Temperature dependences of C_{11} and C_{44} elastic constants. The solid line is a result of calculations of the C_{11} elastic constant from the data obtained in the 180° scattering geometry (see the text).

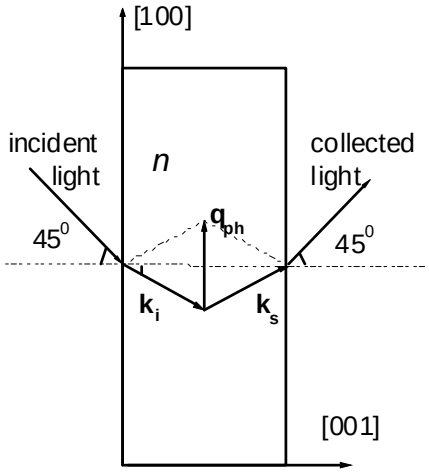

Fig. 1 to paper " Anomalous behavior of acoustic phonons velocity…" by S.G. Lushnikov et.al.

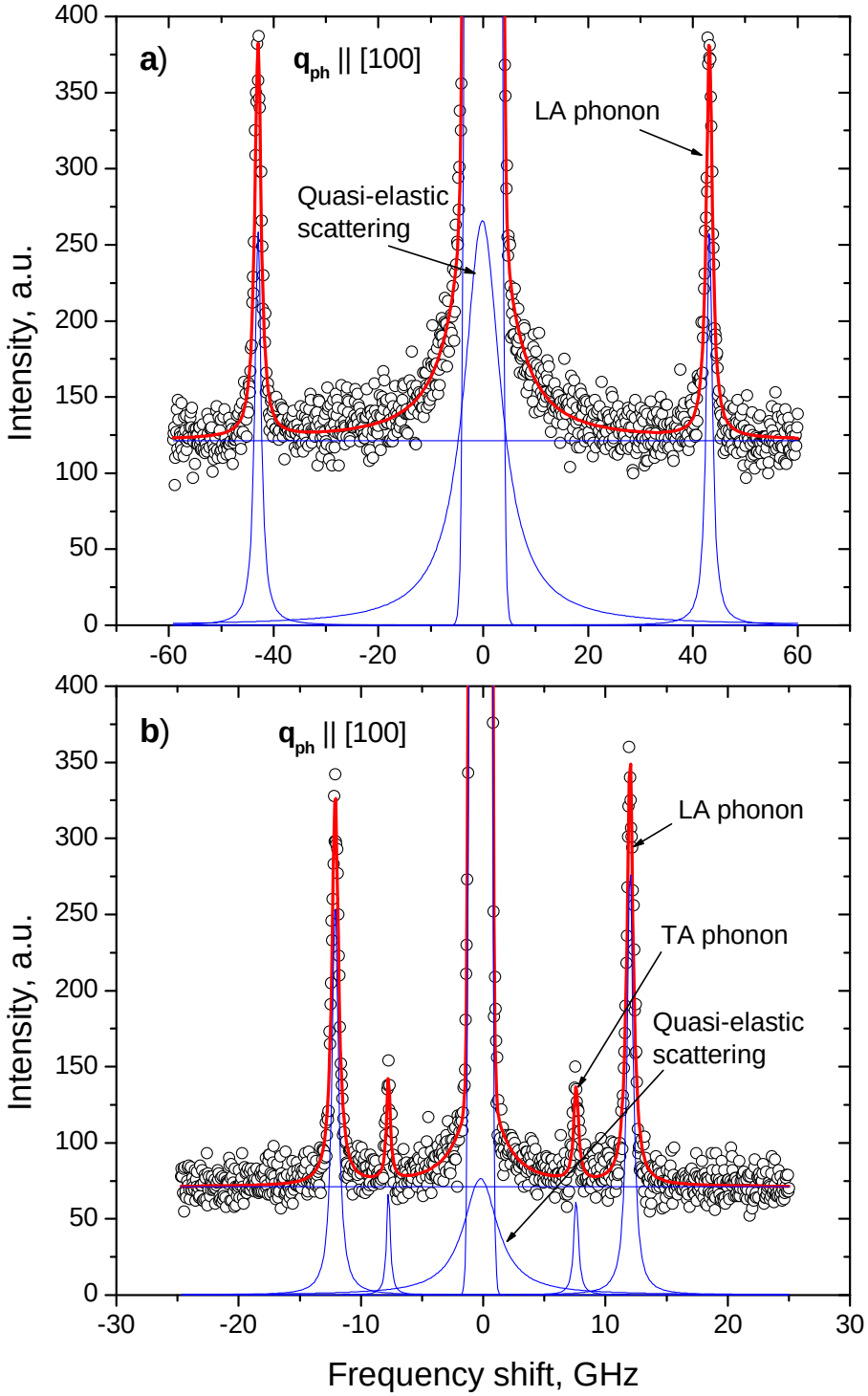

Fig. 2 to paper " Anomalous behavior of acoustic phonons velocity…" by S.G. Lushnikov et.al.

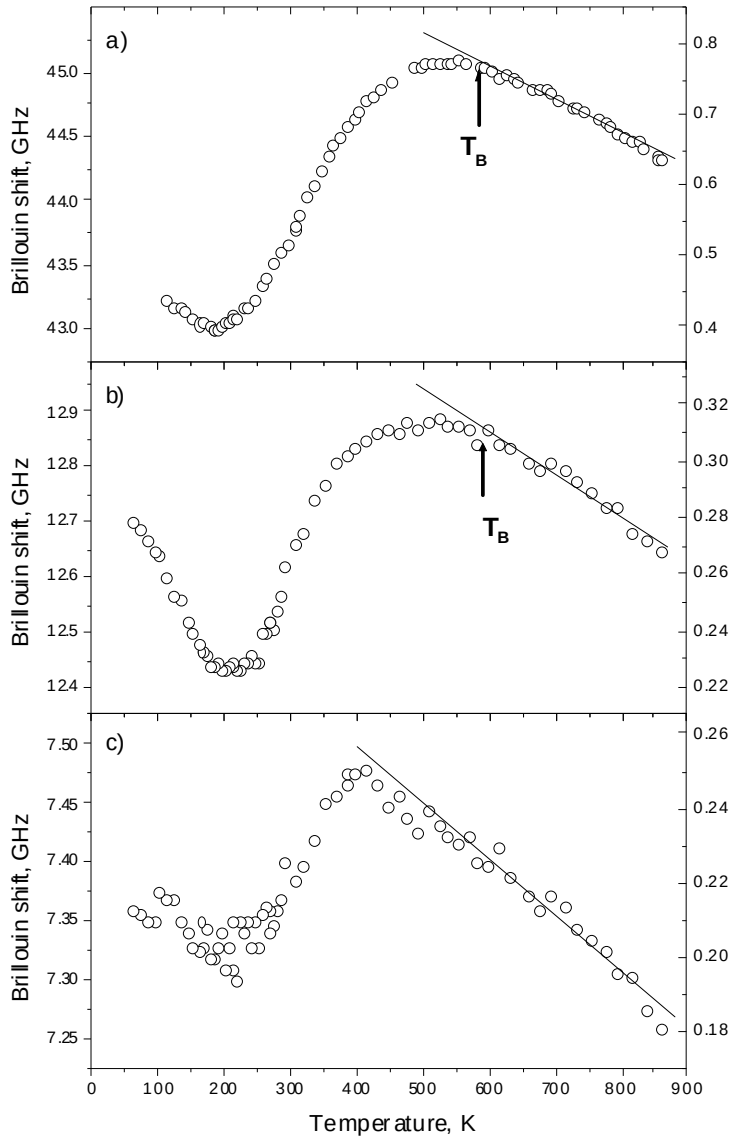

Fig. 3 to paper " Anomalous behavior of acoustic phonons velocity…" by S.G. Lushnikov et.al.

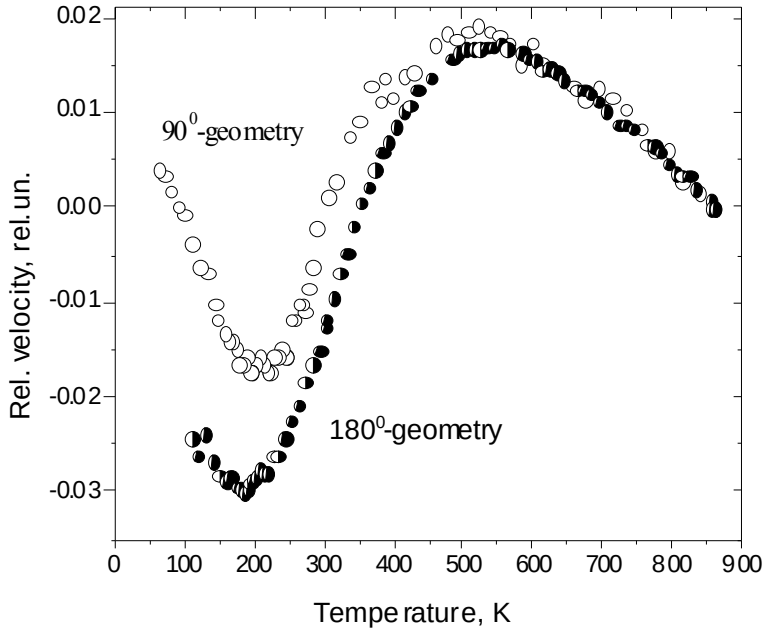

Fig. 4 to paper " Anomalous behavior of acoustic phonons velocity…" by S.G. Lushnikov et.al.

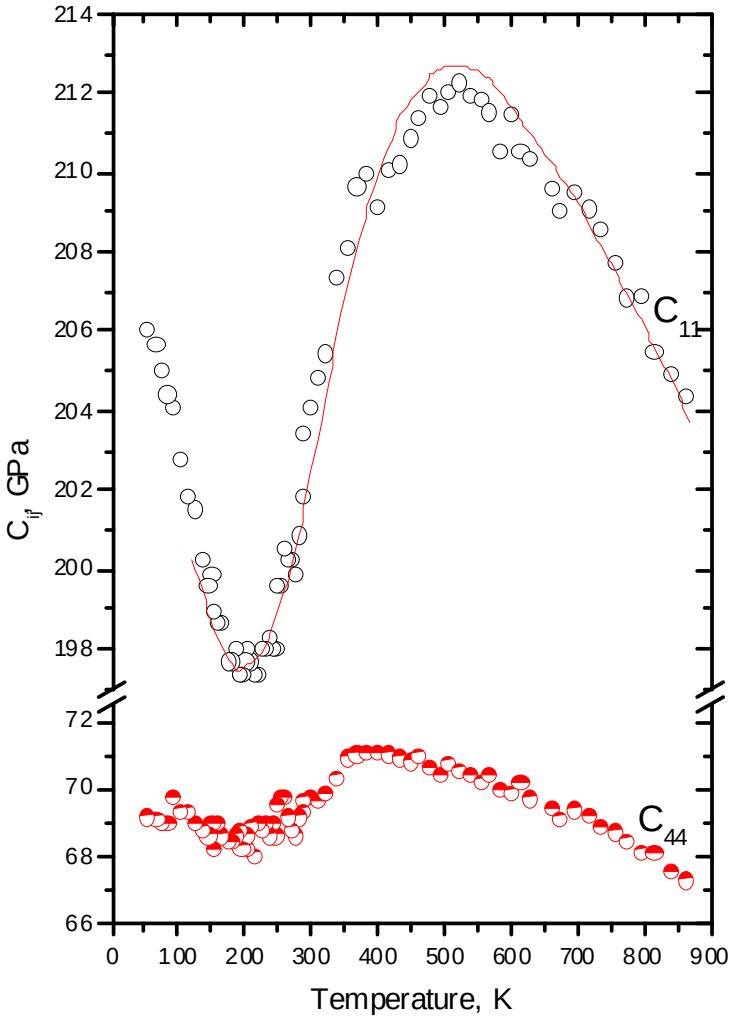

Fig. 5 to paper " Anomalous behavior of acoustic phonons velocity…" by S.G. Lushnikov et.al.